

Identifying and Transferring Reasoning-Critical Neurons: Improving LLM Inference Reliability via Activation Steering

Fangan Dong¹, Zuming Yan¹, Xuri Ge¹, Zhiwei Xu¹, Mengqi Zhang¹, Xuanang Chen², Ben He³, Xin Xin¹, Zhumin Chen¹, Ying Zhou^{1*}

¹Shandong University

²Institute of Software, Chinese Academy of Sciences

³University of Chinese Academy of Sciences

fangan.dong@mail.sdu.edu.cn, yingzhou@sdu.edu.cn

Abstract

Despite the strong reasoning capabilities of recent large language models (LLMs), achieving reliable performance on challenging tasks often requires post-training or computationally expensive sampling strategies, limiting their practical efficiency. In this work, we first show that a small subset of neurons in LLMs exhibits strong predictive correlations with reasoning correctness. Based on this observation, we propose **AdaRAS** (**A**daptive **R**easoning **A**ctivation **S**teering), a lightweight test-time framework that improves reasoning reliability by selectively intervening on neuron activations. AdaRAS identifies Reasoning-Critical Neurons (RCNs) via a polarity-aware mean-difference criterion and adaptively steers their activations during inference, enhancing incorrect reasoning traces while avoiding degradation on already-correct cases. Experiments on 10 mathematics and coding benchmarks demonstrate consistent improvements, including over 13% gains on AIME-24 and AIME-25. Moreover, AdaRAS exhibits strong transferability across datasets and scalability to stronger models, outperforming post-training methods without additional training or sampling cost¹.

1 Introduction

Recent large language models (LLMs) (Jaech et al., 2024; Yang et al., 2025a; DeepSeek-AI, 2025) have demonstrated strong capability across a wide range of natural language processing tasks. In particular, test-time scaling (Wei et al., 2022; Brown et al., 2024) has improved LLM performance by allocating additional computation at inference, enabling applications in mathematical problem solving (Guan et al., 2025; Muennighoff et al., 2025), code generation (Shi et al., 2024; Jain et al., 2025), and spatial reasoning (Fu et al., 2024). Despite

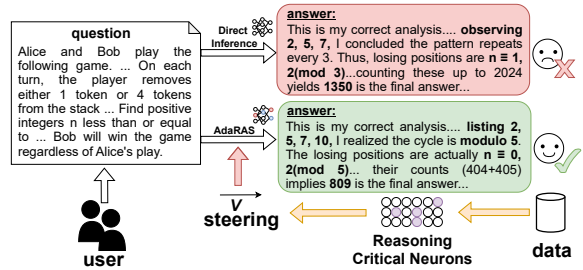


Figure 1: An example of activation steering correcting an erroneous reasoning trajectory.

these advances, reliable reasoning remains challenging even for state-of-the-art models, and most improvements rely on post-training methods (Shao et al., 2024; Cui et al., 2025; Yu et al., 2025) or costly test-time strategies such as prompt engineering (Tian et al., 2024; Saha et al., 2025), self-consistency (Wang et al., 2023; Qiu et al., 2024), or multi-step calibration (Cobbe et al., 2021; Li et al., 2025; Snell et al., 2024). While effective, these approaches treat LLMs as black boxes, incur substantial inference overhead, and offer limited insight into the sources of reasoning errors.

Recent research works in activation engineering (Turner et al., 2023) provides an internal alternative, showing that selectively manipulating activations in attention heads (Li et al., 2023b) or MLP neurons (Rimsky et al., 2024) can control model behaviors, such as truthfulness (Marks and Tegmark, 2023), refusal (Lee et al., 2025), or reducing bias (Lu and Rimsky, 2024), without modifying model parameters or increasing inference cost. This suggests that internal activations encode functionally specialized signals that can be directly leveraged for controllable behavior. However, reasoning reliability is a fundamentally different problem: it is a trajectory-level property requiring temporally coherent, multi-step inference with long-range dependencies, rather than adjustment of a single output attribute. It therefore remains unclear

*Corresponding author.

¹The code and data are available at <https://github.com/cat-sk/AdaRAS>

whether existing activation engineering techniques can identify and enhance the internal mechanisms underlying reasoning correctness. This raises a central question: *Can activation-level interventions improve LLM reasoning reliability?*

To address this question, we first examine whether reasoning correctness can be inferred via internal activations. Inspired by probing studies of LLMs (Gurnee et al., 2023), a pilot analysis reveals that a small subset of MLP neurons exhibits polarized activations between correct and incorrect reasoning trajectories, and that these activations are predictive of reasoning outcomes. Building by this observation, we propose AdaRAS, an adaptive activation steering framework for test-time reasoning enhancement. AdaRAS identifies RCNs by contrasting activations from correct and incorrect samples and applies polarity-based filtering to obtain a sparse, functionally consistent neuron set. During inference, AdaRAS selectively intervenes on these RCNs only when a trajectory is likely incorrect, enabling targeted correction without degrading already-correct one. Experiments on ten mathematic and coding benchmarks show that AdaRAS consistently improves accuracy across models, generalizes across tasks and datasets, and requires no additional training or sampling.

The contributions of this paper are threefold: 1) To our knowledge, we present the first systematic evidence that reasoning correctness can be predicted and improved through neuron interventions, establishing activation steering as a viable tool for enhancing LLM reasoning. 2) We introduce AdaRAS, a parameter-free, test-time activation steering framework that consistently enhances reasoning performance and transfers across tasks and datasets. 3) We provide mechanistic insights showing that AdaRAS stabilizes latent reasoning trajectories while preserving semantic representations, enabling plug-and-play deployment.

2 Preliminaries

In this section, we present preliminary probing results showing that specific neuron activations are predictive of reasoning correctness, which motivates the design of our proposed AdaRAS.

2.1 Task Formulation

We first define *Reasoning-Critical Neurons (RCNs)* as neurons who positively contribute to correct reasoning outcomes. Given a dataset $D = \{(x_i, y_i)\}$

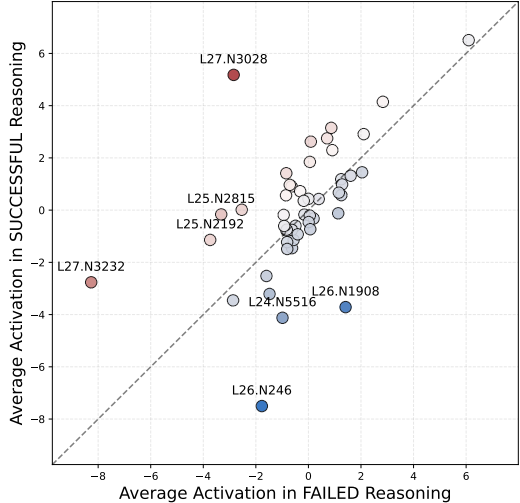


Figure 2: Comparison of activations of key neurons under successful and failed reasoning on AIME.

and a reasoning language model \mathcal{M} , we denote by r_i the model-generated reasoning trace for input x_i , and by a_i the final answer extracted from r_i . We define a binary correctness label $c_i = \mathbb{I}[a_i = y_i]$, which serves as the target signal throughout this work. Architecturally, the model \mathcal{M} consists of L Transformer decoder layers. Following prior work (Geva et al., 2021; Meng et al., 2022), we focus on the MLP blocks, which are widely believed to encode high-level semantic patterns. Specifically, we take the intermediate activation for each MLP block as the internal representation.

2.2 LLM Reasoning Signatures

Motivated by recent advances in LLM interpretability (Belinkov, 2022; Gurnee et al., 2023), we ask whether reasoning correctness can be inferred directly from intermediate neuron activations at test time. As a preliminary study, we probe last-token activations of Qwen3 series models (Yang et al., 2025a) on mathematic datasets (i.e., AIME and AMC-12) to assess their predictive power for reasoning reliability. In contrast to prior work on stylistic control or knowledge editing, we focus on identifying neurons that are specifically predictive of reasoning correctness. Detailed experimental setups are provided in the Appendix A.

Finding 1. LLM reasoning traces leading to correct versus incorrect answers exhibit distinct activation patterns. As shown in Figure 2, we compare the mean activations of highly contrastive neurons under successful and failed reasoning. Notably, the 3028-th neuron in layer 27 shows substan-

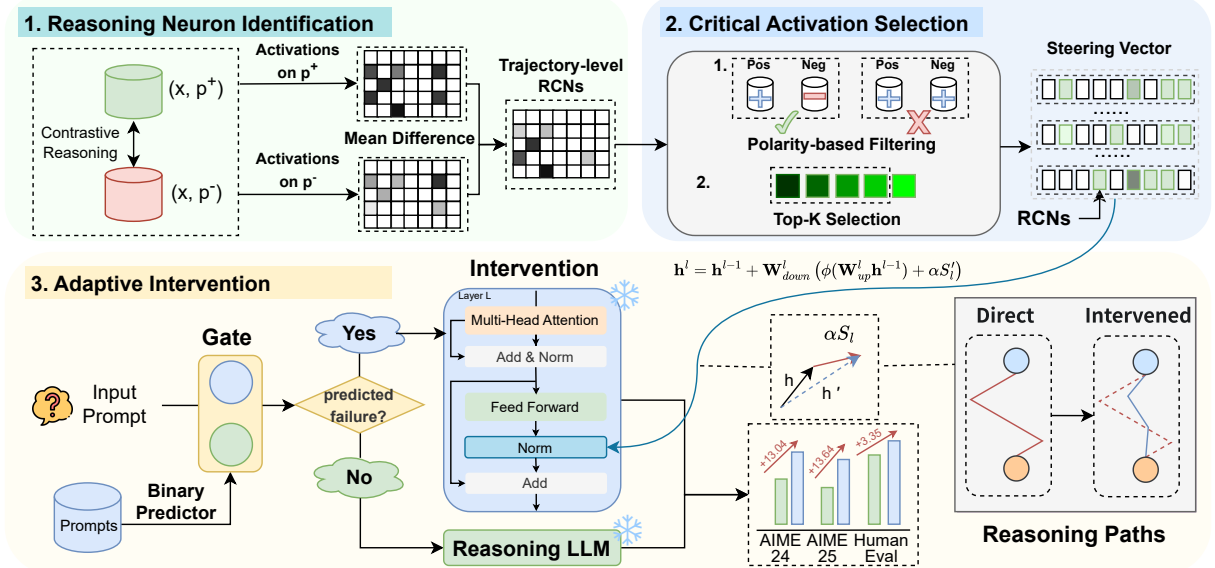


Figure 3: Overview of AdaRAS: (1) reasoning neuron identification (§3.1), which identifies critical neurons by measuring global activation differences between contrastive reasoning trajectories; (2) critical activation selection (§3.2), which further refines RCNs based on activation polarity variations; (3) adaptive intervention (§3.3), which enhances the reliability of steering by predicting reasoning failures and performing adaptive interventions.

Table 1: AUROC of probing classifiers trained on last-token activations for predicting reasoning correctness.

Dataset	Model	AUROC
AIME (24+25)	Qwen3-1.7B	0.7639
	Qwen3-4B	0.7153
AMC-12	Qwen3-1.7B	0.7091
	Qwen3-4B	0.6727

tially higher activation during successful reasoning, whereas the 246-th and 1908-th neurons in layer 26 exhibit the opposite trend. This indicates that specific neurons capture informative signals associated with reasoning success at test time.

Finding 2. Token-level neuron activations are predictive of the final correctness of LLM reasoning. As reported in Table 1, probing classifiers trained solely on last-token activations achieve AUROC scores around 0.7 across two datasets and two models, reaching up to 0.76 on AIME with the Qwen3-1.7B model. These observations suggest that neuron activation states are systematically correlated with reasoning outcomes.

3 Methodology

Figure 3 overviews our AdaRAS framework. First, we identify RCNs by contrasting activation patterns from correct and incorrect reasoning samples

(§3.1). Then, we apply sparse activation steering to selectively intervene on these neurons (§3.2). To avoid perturbing already-correct reasoning, we introduce an adaptive intervention strategy that conditionally modulates activations at test time (§3.3). Finally, we describe the construction of parallel reasoning traces used in our experiments (§3.4).

3.1 Reasoning Neuron Identification

We identify reasoning-critical neurons (RCNs) by directly contrasting activation patterns between correct and incorrect reasoning trajectories. While probing-based methods can assign neuron importance via classifier weights, we find them unreliable in practice due to their sensitivity to feature selection and dependence on probe generalization. Following prior works (Rimsky et al., 2024), we therefore adopt a probing-free, activation-level criterion based on mean activation differences.

Let $a_i^l(t)$ denote the activation value of neuron i at layer l for token t . Given paired correct and incorrect reasoning traces $\mathcal{P} = \{(p_k^+, p_k^-)\}_{k=1}^N$, we define the reasoning-critical score of neuron (l, i) as the difference in mean activations:

$$S(l, i) = \mathbb{E}_{k \sim [N]} \left[\mu(a_i^l, p_k^+) - \mu(a_i^l, p_k^-) \right],$$

$$\mu(a, p) \triangleq \frac{1}{|p|} \sum_{t \in p} a(t), \quad (1)$$

where $|p|$ denotes the length of the reasoning trace.

Unlike prior works (Rimsky et al., 2024) which adopt token-level MD applied to the final answer, this global formulation captures sustained activation patterns accumulated throughout the reasoning process. Specifically, for each layer l , the scores of all neurons form a layer-wise vector $\mathbf{S}_l = [S(l, 1), \dots, S(l, d)]^\top$, which serves as the steering direction for test-time intervention.

3.2 Critical Activation Selection

From preliminary results, our key observation is that correct reasoning is supported by structured activation patterns formed by a small subset of neurons, rather than uniformly distributed across entire layers. Therefore, instead of intervening at the layer level, we perform neuron-level selection and steering. Specifically, most modern LLMs, such as LLaMA and Qwen, employ SwiGLU activations (Shazeer, 2020), whose signed output is necessary for representations learning (Huang, 2024). Our empirical analysis also reveals that neurons whose average activation polarity differs between correct and incorrect reasoning trajectories are particularly discriminative (see 4.4 for detailed results). Intuitively, such polarity reversals indicate neurons that actively support or suppress valid reasoning, depending on the reasoning outcome.

Formally, for each neuron (l, i) , we retain it for steering only if

$$\mathbb{E}_k \left[\mu(a_i^l, p_k^+) \right] \cdot \mathbb{E}_k \left[\mu(a_i^l, p_k^-) \right] < 0, \quad (2)$$

i.e., its mean activation exhibits a sign flip between correct and incorrect traces. This polarity-based filtering yields a sparse candidate set of RCNs. We then rank the retained neurons by the magnitude of their importance scores $|S(l, i)|$ and select the top- K neurons to construct a sparse steering vector \mathbf{S}'_l for each layer. The steering strength is controlled by a positive scalar $\alpha \in [0, \infty]$. Activation steering is applied within the MLP block of the LLM:

$$\mathbf{h}^l = \mathbf{h}^{l-1} + \mathbf{W}_{down}^l \left(\phi(\mathbf{W}_{up}^l \mathbf{h}^{l-1}) + \alpha \mathbf{S}'_l \right), \quad (3)$$

where \mathbf{S}'_l is constructed once from a reference dataset and applied uniformly at each decoding step during test-time inference.

3.3 Adaptive Intervention Strategy

Our early experiments shown a trade-off in activation steering: while it effectively rectifies incorrect reasoning, it inadvertently degrade performance

on some originally correct samples. To address this, we introduce a lightweight failure prediction module that adaptively gates steering at test time. Specifically, we formulate a prediction task to estimate whether the base model can correctly answer a given input. The predictor operates on early neuron activations induced by the input prompt, which capture the model’s initial reasoning state. To reduce dimensionality, we select a small set of activations using F -statistics method as the input features. A attention-based classifier is then trained on these features and achieves an AUROC of 0.8347 on AIME dataset, which further supports our insights that there exists a strong correlation between activation patterns and reasoning outcomes. During inference, the predictor serves as a gate: AdaRAS is applied only when a reasoning failure is predicted. This adaptive intervention improves overall reasoning reliability while preserving performance on inputs that are already correctly handled.

3.4 Contrastive Data Construction

As mentioned in Section 3.1, identifying RCNs requires contrastive reasoning traces that share the same input but differ in outcome correctness. To this end, we construct paired positive and negative reasoning trajectories via self-sampling. For each input prompt, we sample multiple reasoning trajectories using high-temperature decoding and partition them into positive and negative sets based on answer correctness. Contrastive pairs are then formed by matching traces with identical inputs but opposite outcomes. Aggregating all pairs yields a contrastive reasoning set $\mathcal{P} = \{(p^+, p^-)\}$, which is used to identify and transfer RCN activations.

4 Experiments

4.1 Experimental Setup

Dataset. We evaluate AdaRAS on mathematics and coding benchmarks, as both tasks require coherent reasoning traces. We consider 10 widely used datasets. For those without an official training split, we sample a small subset of the test data as a probing set. For each probing sample, we generate 4 paired of positive and negative reasoning traces, which are used for RCNs identification. The remaining samples are reserved for test-time steering evaluation, with no overlap with probing set. Table 8 summarizes the statistics of these datasets.

Baseline. We compare AdaRAS with the following baselines: (1) **Chain-of-Thought (CoT)**. We

Table 2: Experimental results on mathematics and coding benchmarks. We compare AdaRAS with probing-based steering and post-training baselines, evaluated using the Accuracy metric. **Bold** numbers denote the best performance on each dataset. **Red subscripts** indicate the improvement of AdaRAS over the CoT prompting.

Task	Dataset	Post-training				Steering	
		CoT	R1-Distill	Nemotron	OpenThinker	Probing	AdaRAS
Math	AIME-24	47.83	34.78	39.13	26.08	43.48	60.87 _{+13.04}
	AIME-25	40.91	22.73	40.91	50.00	50.00	54.55 _{+13.64}
	AIME-Extend	47.33	21.33	47.33	42.67	48.00	52.67 _{+5.34}
	MATH-500	84.80	66.20	85.40	82.00	85.40	86.40 _{+1.60}
	GSM8K	88.32	72.93	87.57	67.55	88.32	89.08 _{+0.76}
	AMC-12	65.93	41.76	65.93	53.85	73.63	70.33 _{+4.40}
Code	HumanEval	77.18	45.64	57.72	59.06	77.85	79.19 _{+2.01}
	HumanEval+	69.80	42.95	51.68	53.69	72.48	73.15 _{+3.35}
	MBPP	68.78	42.59	53.97	35.71	70.37	72.22 _{+3.44}
	MBPP+	58.20	37.30	43.92	30.95	59.52	60.58 _{+2.38}

include the vanilla CoT prompting performance of Qwen3-1.7B as a baseline, on which AdaRAS is applied. (2) **Post-trained reasoning models.** Post-training methods (e.g., SFT, PPO, GRPO) are known to enhance model’s reasoning performance. We therefore consider three publicly available post-trained models with comparable scales: DeepSeek-R1-Distill-Qwen-1.5B (DeepSeek-AI, 2025), OpenThinker-3-1.5B (Guha et al., 2025), and OpenReasoning-Nemotron-1.5B (Ahmad et al., 2025). (3) **Probing-based steering.** We use the weights of the probing classifier trained in §2.2 as neuron importance scores, select the same number of top-ranked neurons as in AdaRAS, and perform activation addition steering (Turner et al., 2023) accordingly. This baseline is denoted as *Probing*.

Evaluation. We use greedy decoding (i.e., generation temperature = 0) for all methods to ensure reproducibility. Following prior work, we report Accuracy as the evaluation metric across all datasets.

4.2 Main Results

Table 2 reports the reasoning performance improvement of AdaRAS on ten benchmarks, compared against the base model and post-training methods.

AdaRAS consistently improves reasoning correctness across all datasets, even surpassing post-trained LLMs. On average, AdaRAS achieves an improvement of $\sim 5\%$ over CoT-based inference. Notably, on the challenging AIME-25 benchmark, AdaRAS yields a substantial gain of 13.64%,

surpassing all existing open-source post-trained models of comparable scale. We further observe that the performance gains introduced by AdaRAS are more pronounced on hard reasoning benchmarks, such as AIME and AMC. On these datasets, AdaRAS achieves an average improvement of 9.11%, compared to a more modest gain of 2.26% on relatively easier benchmarks. These results suggest that steering RCN activations toward favorable states can substantially enhance the reliability of the generation process, particularly for complex and cognitively demanding reasoning tasks.

Probing-based activation steering is inherently unstable. As shown in Table 2, vanilla probing-based steering yields mixed results across datasets. While it achieves notable gains on AMC-12, even surpassing AdaRAS, it fails to generalize and can be detrimental on more challenging benchmarks. In particular, on AIME-24, probing-based steering degrades accuracy by 4.35% compared to the unsteered CoT baseline. These results indicate that naive probing-based approaches are highly sensitive to neuron selection, and may harm reasoning performance without adaptive intervention mechanisms, which are explicitly addressed in AdaRAS.

4.3 Generalizability

Tables 3 and 4 further evaluate AdaRAS in the views of transferability and generalization, covering cross-dataset setting and larger model scale.

Table 3: Transferability results of AdaRAS across datasets. We compare in-domain steering using RCNs identified on each dataset (*ID. RCNs*) with cross-dataset steering using RCNs identified on AIME (*AIME-RCNs*).

Dataset	ID. RCNs	AIME-RCNs
MATH-500	86.40	87.40
GSM8K	89.08	89.39
AMC-12	70.33	71.43
HumanEval	79.19	80.54
HumanEval+	73.15	73.15
MBPP	72.22	72.75
MBPP+	60.58	61.11

Table 4: Scalability results of AdaRAS on Qwen3-4B. We evaluate AdaRAS on a larger base model using cross-dataset steering with RCNs identified on AIME.

Dataset	Qwen3-4B	+AdaRAS
AIME-24	56.52	60.87
AIME-25	59.09	72.73
AIME-Extend	68.67	76.67
MATH-500	90.00	91.20
GSM8K	92.72	93.93
AMC-12	76.92	80.22
HumanEval	91.28	92.62
HumanEval+	81.88	84.56
MBPP	79.37	82.28
MBPP+	68.78	69.31

RCNs exhibit strong cross-dataset and cross-task transferability. As shown in Table 3, compared to using dataset-specific RCNs, we observe that cross-dataset activation steering with RCNs identified on AIME consistently yields better performance, resulting in small but stable gains, within 1%, across all evaluated datasets. Notably, these RCNs also transfer across task domains: when applied to coding benchmarks, they continue to improve performance. These results support our motivation for identifying RCNs and suggest that such neurons capture task-agnostic reasoning mechanisms. In particular, RCNs identified from more challenging tasks appear to generalize broadly to diverse reasoning settings.

AdaRAS scales effectively to stronger reasoning models. Table 4 shows that AdaRAS continues to yield performance improvements when applied to the larger and more capable reasoning

Table 5: Ablation results of key components in AdaRAS. *Random Steering* applies steering to randomly sampled neurons. *AdaRAS w/o MD* reduces the method to probing-based neuron importance estimation, instead of Mean Difference designed in §3.1. *AS* and *AI* denote Activation Selection and Adaptive Intervention, corresponding to the designs in §3.2 and §3.3, respectively.

Method	AIME-24	AIME-25
Qwen3-1.7B	47.83	40.91
Random Steering	34.78	27.27
AdaRAS w/o MD	43.48	50.00
AdaRAS w/o AS	52.17	45.45
AdaRAS w/o AI	56.52	45.45
AdaRAS	60.87	54.55

model. Even when the base model already achieves high accuracy, whereas Qwen3-4B surpasses 90% accuracy on relatively easier benchmarks such as MATH-500, GSM8K, and HumanEval, AdaRAS still delivers consistent accuracy gains of around 1%. Notably, on more challenging datasets such as AIME, the improvements are more pronounced, mirroring the trends observed in previous experiments. Overall, these results indicate that AdaRAS acts as a complementary test-time intervention, providing consistent gains even as the base model’s reasoning capability improves.

4.4 Ablation Studies

Table 5 reports the ablation results for AdaRAS. (1) Random Steering consistently degrades performance, indicating that indiscriminate neuron intervention is harmful. (2) Removing the MD-based estimation results in the sharpest decline on AIME-24 (i.e., 60.87% → 43.48%), dropping even below the unsteered baseline. This underscores the necessity of MD for accurately identifying RCNs. (3) Disabling polarity-based activation selection causes an approximate 10% accuracy drop on both AIME-24 and AIME-25, highlighting the importance of discriminative activation polarity; limited by space, further analysis is in Appendix E.2. (4) Omitting adaptive intervention degrades overall performance by interfering with originally correct reasoning trajectories. Overall, all components are essential to the effectiveness of AdaRAS.

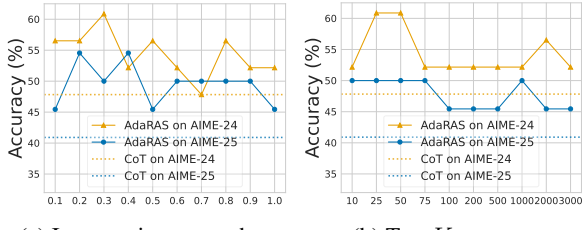


Figure 4: Effect of hyperparameter.

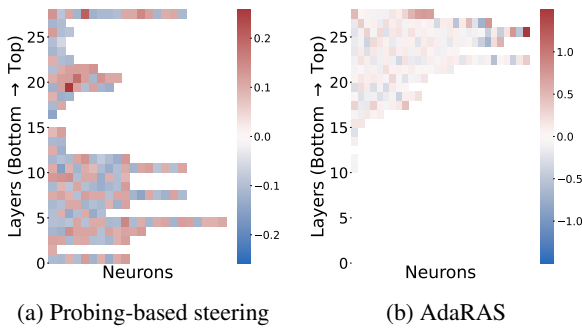


Figure 5: Visualization of activation shifts induced by steering. Neurons are sorted by their indices in layer, and unsteered neurons are omitted for clarity.

5 Analysis

5.1 Effect of Hyperparameter

To further examine the design of AdaRAS, we analyze its hyperparameters. Specifically, we vary the intervention strength α in Eq. 3 within $[0, 1]$, which controls the magnitude of activation shifts toward the identified RCNs. We also vary the number of selected neurons to empirically assess the sparsity assumption of RCNs introduced in §3.2.

Effect of intervention strength. As shown in Figure 4a, AdaRAS achieves peak performance at $\alpha = 0.3$ on AIME-24 and $\alpha = 0.4$ on AIME-25. Increasing α beyond these values leads to performance decline, suggesting that excessive intervention interferes with the model’s reasoning process. Notably, performance drops to the unsteered baseline only when $\alpha = 0.7$ on AIME-24. This suggests that AdaRAS is relatively robust to suboptimal hyperparameter choices and does not significantly harm the original reasoning capability under most settings.

Effect of top- K RCNs selection. In the ablation study, we have shown that removing AdaRAS’s polarity-aware filtering of RCNs leads to degraded steering performance. Figure 4b further reveals the sparse nature of RCNs. Specifically, steering performance improves as more RCNs are intervened

on, peaks at approximately top-50 neurons (about 0.03% of all neurons), and degrades thereafter. In particular, when intervening on top-2000 neurons (about 1.20%), performance on AIME-24 drops by around 6% compared to performance at top-50. These results provide strong empirical evidence supporting our hypothesis in §3.2 that RCNs are sparse and highly selective, and that indiscriminate intervention on a large set of neurons can be detrimental to reasoning performance.

5.2 Visualization of Steering

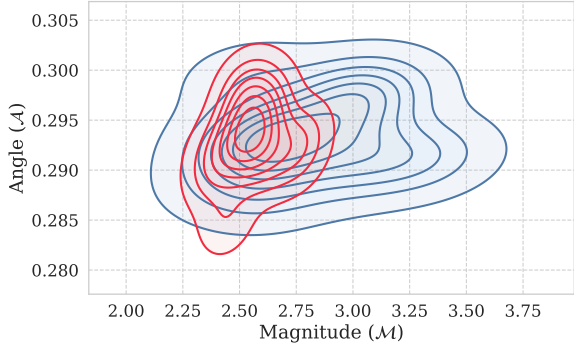
We visualize the effects of AdaRAS from neuron-level activation shifts to trajectory-level features of reasoning paths.

AdaRAS mainly intervenes on later layer neurons.

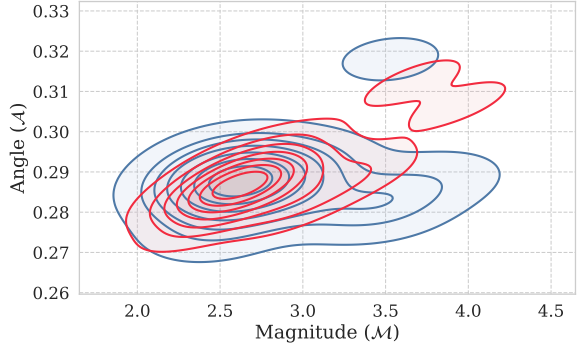
Figure 5 compares activation shifts of RCNs induced by vanilla probing-based steering and AdaRAS on AIME-24 and AIME-25, where shifts are computed as the difference between mean neuron activations before and after steering. Compared to probing-based methods, which introduce widespread changes in early layers, AdaRAS concentrates its interventions on later layers and induces substantially smaller activation shifts, with most values tightly centered around zero. This observation aligns with prior findings (Biran et al., 2024) that later layer neurons are more important for multi-hop reasoning.

AdaRAS stabilizes latent reasoning trajectories without altering semantic modeling.

To further analyze the effect of AdaRAS on the reasoning process, we examine the stability of latent reasoning paths. Following Wang et al. (2025b), we compute two trajectory-level features from layer-wise activations: **magnitude** and **angle**, which capture reasoning path curvature and semantic modeling level, respectively. Formal definitions are provided in the Appendix D due to space limitations. As shown in Figure 6, under both in-domain and cross-dataset steering, steered samples exhibit significantly lower and more concentrated magnitude values than unsteered samples, indicating that AdaRAS reduces fluctuations in latent reasoning trajectories. In contrast, the angle metric remains largely unchanged, suggesting that AdaRAS stabilizes reasoning dynamics without substantially altering semantic modeling behavior.



(a) AIME (In-domain steering)



(b) MBPP (Cross-task steering)

Figure 6: Feature distribution discrepancy of activations *before* and *after* intervention. The x-axis denotes the magnitude feature, and the y-axis denotes the angle feature of activations. Larger values indicate greater deviations in activation space. Detailed definitions are provided in Appendix D.

6 Related Works

Reasoning Reliability. Improving reasoning reliability in LLMs has been widely studied via test-time scaling. Prior work achieves performance gains via post-training methods (Ouyang et al., 2022; Lightman et al., 2024; Shao et al., 2024) or costly test-time techniques, like prompt engineering (Wei et al., 2022; Tian et al., 2024), self-consistency (Wang et al., 2023; Saunders et al., 2022), and multi-step calibration (Li et al., 2025; Snell et al., 2024). Other approaches focus on the token or latent level, including redundancy pruning (Xia et al., 2025), optimization of high-entropy tokens (Wang et al., 2025a; Qian et al., 2025), and latent-space reasoning (Chen et al., 2025b; Wang et al., 2025b). Most closely related to our work, Yang et al. (2025b) attributes reasoning errors to high-entropy tokens and improves performance via token-level entropy-based guidance during inference. In contrast, we intervene at the neuron activation level, which is lightweight and more transferable, yielding stronger gains across models, and is fully complementary to token-level methods.

Mechanistic Interpretability. Recent studies have advanced the understanding of transformer-based language models through techniques such as vocabulary projection (Belrose et al., 2023), probing classifiers (Belinkov, 2022; Gurnee et al., 2023), and sparse autoencoders (Bricken et al., 2023; Xin et al., 2025). These approaches show that specific neurons could encode semantical features, including truthfulness (Burns et al., 2023; Marks and Tegmark, 2023), sentiment (Tigges et al., 2023), refusal (Arditi et al., 2024), and stylistic attributes (Li et al., 2023a; Stolfo et al., 2024;

Zou et al., 2023; Rimsky et al., 2024). Building on these insights, a growing body of work explores modifying activations during inference to steer model behavior, achieving regulation of personality traits (Chen et al., 2025a), improved instruction following (Stolfo et al., 2025; Liu et al., 2024), and editing of factual knowledge (Subramani et al., 2022; Hernandez et al., 2023). Inspired by some of these works, we derive intervention signals from contrastive reasoning traces that differ in outcome correctness. However, whereas existing work primarily targets output-level behaviors, we focus on trajectory-level reasoning, enabling interventions to be identified offline and applied at inference time without task-specific retraining.

7 Conclusion

In this work, we propose AdaRAS, an inference-time activation steering framework for improving reasoning reliability in LLMs. We first demonstrate that reasoning correctness is strongly associated with a small subset of neurons. AdaRAS identifies these reasoning-critical neurons via mean activation differences between correct and incorrect reasoning trajectories, and further refines them with polarity-based activation filtering. AdaRAS then applies an adaptive intervention to selectively steer neuron activations during inference. Extensive experiments across ten reasoning benchmarks show that AdaRAS consistently improves accuracy without additional computation cost, and the identified neurons transfer effectively across tasks. Finally, trajectory-level analyses using latent reasoning features provide mechanistic evidence that AdaRAS stabilizes reasoning paths without affecting seman-

tic modeling level of LLMs.

Limitations

Although effective, our work has several limitations. First, our analysis focuses on the Qwen3 series models and STEM benchmarks. Extending the evaluation to a broader range of model architectures and complex reasoning settings (e.g., spatial or multi-hop reasoning) is necessary to assess the generalizability of our findings for future work. Second, as with many interpretability studies, our approach relies on constructing contrastive data pairs. This requirement may limit applicability to models at capability extremes, where obtaining paired correct and incorrect reasoning trajectories is non-trivial. Exploring alternative data construction strategies that relax this requirement is an important direction for future work. Third, to identify RCNs, we focus on neuron-level activations with the mean difference metric. Future work could incorporate other advanced techniques, such as sparse autoencoders or vocabulary projection analyses, to further elucidate the mechanistic underpinnings of RCNs.

Ethics Statement

This work investigates inference-time activation steering methods for improving the reasoning reliability of large language models. All experiments are conducted using publicly available models and open-source benchmarks. The study does not involve the collection of personal data, human subjects, or real-world deployment, etc.

References

Wasi Uddin Ahmad, Sean Narendhiran, Somshubra Majumdar, Aleksander Ficek, Siddhartha Jain, Jocelyn Huang, Vahid Noroozi, and Boris Ginsburg. 2025. [Opencodereasoning: Advancing data distillation for competitive coding](#). *CoRR*, abs/2504.01943.

Andy Ardit, Oscar Obeso, Aaquib Syed, Daniel Paleka, Nina Panickssery, Wes Gurnee, and Neel Nanda. 2024. [Refusal in language models is mediated by a single direction](#). In *Advances in Neural Information Processing Systems 38: Annual Conference on Neural Information Processing Systems 2024, NeurIPS 2024, Vancouver, BC, Canada, December 10 - 15, 2024*.

Jacob Austin, Augustus Odena, Maxwell Nye, Maarten Bosma, Henryk Michalewski, David Dohan, Ellen Jiang, Carrie Cai, Michael Terry, Quoc Le, and 1 others. 2021. Program synthesis with large language models. *arXiv preprint arXiv:2108.07732*.

Yonatan Belinkov. 2022. [Probing classifiers: Promises, shortcomings, and advances](#). *Comput. Linguistics*, 48(1):207–219.

Nora Belrose, Zach Furman, Logan Smith, Danny Halawi, Igor Ostrovsky, Lev McKinney, Stella Biderman, and Jacob Steinhardt. 2023. [Eliciting latent predictions from transformers with the tuned lens](#). *CoRR*, abs/2303.08112.

Eden Biran, Daniela Gottesman, Sohee Yang, Mor Geva, and Amir Globerson. 2024. [Hopping too late: Exploring the limitations of large language models on multi-hop queries](#). In *Proceedings of the 2024 Conference on Empirical Methods in Natural Language Processing, EMNLP 2024, Miami, FL, USA, November 12-16, 2024*, pages 14113–14130. Association for Computational Linguistics.

Trenton Bricken, Adly Templeton, Joshua Batson, Brian Chen, Adam Jermyn, Tom Conerly, Nick Turner, Cem Anil, Carson Denison, Amanda Askell, Robert Lasenby, Yifan Wu, Shauna Kravec, Nicholas Schiefer, Tim Maxwell, Nicholas Joseph, Zac Hatfield-Dodds, Alex Tamkin, Karina Nguyen, and 6 others. 2023. Towards monosemanticity: Decomposing language models with dictionary learning. *Transformer Circuits Thread*. [Https://transformer-circuits.pub/2023/monosemantic-features/index.html](https://transformer-circuits.pub/2023/monosemantic-features/index.html).

Bradley C. A. Brown, Jordan Juravsky, Ryan Ehrlich, Ronald Clark, Quoc V. Le, Christopher Ré, and Azalia Mirhoseini. 2024. [Large language monkeys: Scaling inference compute with repeated sampling](#). *CoRR*, abs/2407.21787.

Collin Burns, Haotian Ye, Dan Klein, and Jacob Steinhardt. 2023. [Discovering latent knowledge in language models without supervision](#). In *The Eleventh International Conference on Learning Representations, ICLR 2023, Kigali, Rwanda, May 1-5, 2023*. OpenReview.net.

Mark Chen, Jerry Tworek, Heewoo Jun, Qiming Yuan, Henrique Ponde de Oliveira Pinto, Jared Kaplan, Harri Edwards, Yuri Burda, Nicholas Joseph, Greg Brockman, Alex Ray, Raul Puri, Gretchen Krueger, Michael Petrov, Heidy Khlaaf, Girish Sastry, Pamela Mishkin, Brooke Chan, Scott Gray, and 39 others. 2021. [Evaluating large language models trained on code](#). *Preprint*, arXiv:2107.03374.

Runjin Chen, Andy Ardit, Henry Sleight, Owain Evans, and Jack Lindsey. 2025a. [Persona vectors: Monitoring and controlling character traits in language models](#). *CoRR*, abs/2507.21509.

Xinghao Chen, Anhao Zhao, Heming Xia, Xuan Lu, Hanlin Wang, Yanjun Chen, Wei Zhang, Jian Wang, Wenjie Li, and Xiaoyu Shen. 2025b. [Reasoning beyond language: A comprehensive survey on latent chain-of-thought reasoning](#). *CoRR*, abs/2505.16782.

Karl Cobbe, Vineet Kosaraju, Mohammad Bavarian, Mark Chen, Heewoo Jun, Lukasz Kaiser, Matthias Plappert, Jerry Tworek, Jacob Hilton, Reiichiro Nakano, Christopher Hesse, and John Schulman. 2021. [Training verifiers to solve math word problems](#). *CoRR*, abs/2110.14168.

Ganqu Cui, Lifan Yuan, Zefan Wang, Hanbin Wang, Wendi Li, Bingxiang He, Yuchen Fan, Tianyu Yu, Qixin Xu, Weize Chen, Jiarui Yuan, Huayu Chen, Kaiyan Zhang, Xingtai Lv, Shuo Wang, Yuan Yao, Xu Han, Hao Peng, Yu Cheng, and 4 others. 2025. [Process reinforcement through implicit rewards](#). *CoRR*, abs/2502.01456.

DeepSeek-AI. 2025. [Deepseek-r1: Incentivizing reasoning capability in llms via reinforcement learning](#). *CoRR*, abs/2501.12948.

Rao Fu, Jingyu Liu, Xilun Chen, Yixin Nie, and Wenhan Xiong. 2024. [Scene-lilm: Extending language model for 3d visual understanding and reasoning](#). *CoRR*, abs/2403.11401.

Mor Geva, Roei Schuster, Jonathan Berant, and Omer Levy. 2021. [Transformer feed-forward layers are key-value memories](#). In *Proceedings of the 2021 Conference on Empirical Methods in Natural Language Processing, EMNLP 2021, Virtual Event / Punta Cana, Dominican Republic, 7-11 November, 2021*, pages 5484–5495. Association for Computational Linguistics.

Xinyu Guan, Li Lyra Zhang, Yifei Liu, Ning Shang, Youran Sun, Yi Zhu, Fan Yang, and Mao Yang. 2025. [rstar-math: Small llms can master math reasoning with self-evolved deep thinking](#). In *Forty-second International Conference on Machine Learning, ICML 2025, Vancouver, BC, Canada, July 13-19, 2025*. OpenReview.net.

Etash Kumar Guha, Ryan Marten, Sedrick Keh, Negin Raoof, Georgios Smyrnis, Hritik Bansal, Marianna Nezhurina, Jean Mercat, Trung Vu, Zayne Sprague, Ashima Suvarna, Benjamin Feuer, Liangyu Chen, Zaid Khan, Eric Frankel, Sachin Grover, Caroline Choi, Niklas Muennighoff, Shiye Su, and 31 others. 2025. [Openthoughts: Data recipes for reasoning models](#). *CoRR*, abs/2506.04178.

Wes Gurnee, Neel Nanda, Matthew Pauly, Katherine Harvey, Dmitrii Troitskii, and Dimitris Bertsimas. 2023. [Finding neurons in a haystack: Case studies with sparse probing](#). *Trans. Mach. Learn. Res.*, 2023.

Dan Hendrycks, Collin Burns, Saurav Kadavath, Akul Arora, Steven Basart, Eric Tang, Dawn Song, and Jacob Steinhardt. 2021. Measuring mathematical problem solving with the math dataset. *arXiv preprint arXiv:2103.03874*.

Evan Hernandez, Belinda Z Li, and Jacob Andreas. 2023. [Inspecting and editing knowledge representations in language models](#). *arXiv preprint arXiv:2304.00740*.

Allen Hao Huang. 2024. [Expanded gating ranges improve activation functions](#). *CoRR*, abs/2405.20768.

Aaron Jaech, Adam Kalai, Adam Lerer, Adam Richardson, Ahmed El-Kishky, Aiden Low, Alec Helyar, Aleksander Madry, Alex Beutel, Alex Carney, Alex Iftimie, Alex Karpenko, Alex Tachard Passos, Alexander Neitz, Alexander Prokofiev, Alexander Wei, Allison Tam, Ally Bennett, Ananya Kumar, and 80 others. 2024. [Openai o1 system card](#). *CoRR*, abs/2412.16720.

Naman Jain, King Han, Alex Gu, Wen-Ding Li, Fanjia Yan, Tianjun Zhang, Sida Wang, Armando Solar-Lezama, Koushik Sen, and Ion Stoica. 2025. [Livecodebench: Holistic and contamination free evaluation of large language models for code](#). In *The Thirteenth International Conference on Learning Representations, ICLR 2025, Singapore, April 24-28, 2025*. OpenReview.net.

Bruce W. Lee, Inkit Padhi, Karthikeyan Natesan Ramamurthy, Erik Miehling, Pierre L. Dognin, Manish Nagireddy, and Amit Dhurandhar. 2025. [Programming refusal with conditional activation steering](#). In *The Thirteenth International Conference on Learning Representations, ICLR 2025, Singapore, April 24-28, 2025*. OpenReview.net.

Chengpeng Li, Mingfeng Xue, Zhenru Zhang, Jiaxi Yang, Beichen Zhang, Xiang Wang, Bowen Yu, Binyuan Hui, Junyang Lin, and Dayiheng Liu. 2025. [START: self-taught reasoner with tools](#). *CoRR*, abs/2503.04625.

Kenneth Li, Aspen K. Hopkins, David Bau, Fernanda B. Viégas, Hanspeter Pfister, and Martin Wattenberg. 2023a. [Emergent world representations: Exploring a sequence model trained on a synthetic task](#). In *The Eleventh International Conference on Learning Representations, ICLR 2023, Kigali, Rwanda, May 1-5, 2023*. OpenReview.net.

Kenneth Li, Oam Patel, Fernanda B. Viégas, Hanspeter Pfister, and Martin Wattenberg. 2023b. [Inference-time intervention: Eliciting truthful answers from a language model](#). In *Advances in Neural Information Processing Systems 36: Annual Conference on Neural Information Processing Systems 2023, NeurIPS 2023, New Orleans, LA, USA, December 10 - 16, 2023*.

Hunter Lightman, Vineet Kosaraju, Yuri Burda, Harrison Edwards, Bowen Baker, Teddy Lee, Jan Leike, John Schulman, Ilya Sutskever, and Karl Cobbe. 2024. [Let's verify step by step](#). In *The Twelfth International Conference on Learning Representations, ICLR 2024, Vienna, Austria, May 7-11, 2024*. OpenReview.net.

Jiawei Liu, Chunqiu Steven Xia, Yuyao Wang, and Linging Zhang. 2023. [Is your code generated by chat-GPT really correct? rigorous evaluation of large language models for code generation](#). In *Thirty-seventh Conference on Neural Information Processing Systems*.

Sheng Liu, Haotian Ye, Lei Xing, and James Y. Zou. 2024. *In-context vectors: Making in context learning more effective and controllable through latent space steering*. In *Forty-first International Conference on Machine Learning, ICML 2024, Vienna, Austria, July 21-27, 2024*. OpenReview.net.

Dawn Lu and Nina Rimsky. 2024. *Investigating bias representations in llama 2 chat via activation steering*. *CoRR*, abs/2402.00402.

Samuel Marks and Max Tegmark. 2023. *The geometry of truth: Emergent linear structure in large language model representations of true/false datasets*. *CoRR*, abs/2310.06824.

Kevin Meng, David Bau, Alex Andonian, and Yonatan Belinkov. 2022. *Locating and editing factual associations in GPT*. In *Advances in Neural Information Processing Systems 35: Annual Conference on Neural Information Processing Systems 2022, NeurIPS 2022, New Orleans, LA, USA, November 28 - December 9, 2022*.

Niklas Muennighoff, Zitong Yang, Weijia Shi, Xiang Lisa Li, Li Fei-Fei, Hannaneh Hajishirzi, Luke Zettlemoyer, Percy Liang, Emmanuel J. Candès, and Tatsunori Hashimoto. 2025. *s1: Simple test-time scaling*. *CoRR*, abs/2501.19393.

Long Ouyang, Jeffrey Wu, Xu Jiang, Diogo Almeida, Carroll L. Wainwright, Pamela Mishkin, Chong Zhang, Sandhini Agarwal, Katarina Slama, Alex Ray, John Schulman, Jacob Hilton, Fraser Kelton, Luke Miller, Maddie Simens, Amanda Askell, Peter Welinder, Paul F. Christiano, Jan Leike, and Ryan Lowe. 2022. *Training language models to follow instructions with human feedback*. In *Advances in Neural Information Processing Systems 35: Annual Conference on Neural Information Processing Systems 2022, NeurIPS 2022, New Orleans, LA, USA, November 28 - December 9, 2022*.

Chen Qian, Dongrui Liu, Haochen Wen, Zhen Bai, Yong Liu, and Jing Shao. 2025. *Demystifying reasoning dynamics with mutual information: Thinking tokens are information peaks in LLM reasoning*. *CoRR*, abs/2506.02867.

Jiahao Qiu, Yifu Lu, Yifan Zeng, Jiacheng Guo, Jiayi Geng, Huazheng Wang, Kaixuan Huang, Yue Wu, and Mengdi Wang. 2024. *Treebon: Enhancing inference-time alignment with speculative tree-search and best-of-n sampling*. *CoRR*, abs/2410.16033.

Nina Rimsky, Nick Gabrieli, Julian Schulz, Meg Tong, Evan Hubinger, and Alexander Matt Turner. 2024. *Steering llama 2 via contrastive activation addition*. In *Proceedings of the 62nd Annual Meeting of the Association for Computational Linguistics (Volume 1: Long Papers), ACL 2024, Bangkok, Thailand, August 11-16, 2024*, pages 15504–15522. Association for Computational Linguistics.

Swarnadeep Saha, Xian Li, Marjan Ghazvininejad, Jason E. Weston, and Tianlu Wang. 2025. *Learning to plan & reason for evaluation with thinking-llm-as-a-judge*. In *Forty-second International Conference on Machine Learning, ICML 2025, Vancouver, BC, Canada, July 13-19, 2025*. OpenReview.net.

William Saunders, Catherine Yeh, Jeff Wu, Steven Bills, Long Ouyang, Jonathan Ward, and Jan Leike. 2022. *Self-critiquing models for assisting human evaluators*. *CoRR*, abs/2206.05802.

Zhihong Shao, Peiyi Wang, Qihao Zhu, Runxin Xu, Junxiao Song, Mingchuan Zhang, Y. K. Li, Y. Wu, and Daya Guo. 2024. *Deepseekmath: Pushing the limits of mathematical reasoning in open language models*. *CoRR*, abs/2402.03300.

Noam Shazeer. 2020. *GLU variants improve transformer*. *CoRR*, abs/2002.05202.

Quan Shi, Michael Tang, Karthik Narasimhan, and Shunyu Yao. 2024. *Can language models solve olympiad programming?* *CoRR*, abs/2404.10952.

Charlie Snell, Jaehoon Lee, Kelvin Xu, and Aviral Kumar. 2024. *Scaling LLM test-time compute optimally can be more effective than scaling model parameters*. *CoRR*, abs/2408.03314.

Alessandro Stolfo, Vidhisha Balachandran, Safoora Yousefi, Eric Horvitz, and Besmira Nushi. 2025. *Improving instruction-following in language models through activation steering*. In *The Thirteenth International Conference on Learning Representations, ICLR 2025, Singapore, April 24-28, 2025*. OpenReview.net.

Alessandro Stolfo, Ben Wu, Wes Gurnee, Yonatan Belinkov, Xingyi Song, Mrinmaya Sachan, and Neel Nanda. 2024. *Confidence regulation neurons in language models*. In *Advances in Neural Information Processing Systems 38: Annual Conference on Neural Information Processing Systems 2024, NeurIPS 2024, Vancouver, BC, Canada, December 10 - 15, 2024*.

Nishant Subramani, Nivedita Suresh, and Matthew E. Peters. 2022. *Extracting latent steering vectors from pretrained language models*. In *Findings of the Association for Computational Linguistics: ACL 2022, Dublin, Ireland, May 22-27, 2022*, pages 566–581. Association for Computational Linguistics.

Ye Tian, Baolin Peng, Linfeng Song, Lifeng Jin, Dian Yu, Lei Han, Haitao Mi, and Dong Yu. 2024. *Toward self-improvement of llms via imagination, searching, and criticizing*. In *Advances in Neural Information Processing Systems 38: Annual Conference on Neural Information Processing Systems 2024, NeurIPS 2024, Vancouver, BC, Canada, December 10 - 15, 2024*.

Curt Tigges, Oskar John Hollinsworth, Atticus Geiger, and Neel Nanda. 2023. *Linear representations of sentiment in large language models*. *CoRR*, abs/2310.15154.

Alexander Matt Turner, Lisa Thiergart, David Udell, Gavin Leech, Ulisse Mini, and Monte MacDiarmid. 2023. [Activation addition: Steering language models without optimization](#). *CoRR*, abs/2308.10248.

Shenzhi Wang, Le Yu, Chang Gao, Chujie Zheng, Shixuan Liu, Rui Lu, Kai Dang, Xionghui Chen, Jianxin Yang, Zhenru Zhang, Yuqiong Liu, An Yang, Andrew Zhao, Yang Yue, Shiji Song, Bowen Yu, Gao Huang, and Junyang Lin. 2025a. [Beyond the 80/20 rule: High-entropy minority tokens drive effective reinforcement learning for LLM reasoning](#). *CoRR*, abs/2506.01939.

Xuezhi Wang, Jason Wei, Dale Schuurmans, Quoc V. Le, Ed H. Chi, Sharan Narang, Aakanksha Chowdhery, and Denny Zhou. 2023. [Self-consistency improves chain of thought reasoning in language models](#). In *The Eleventh International Conference on Learning Representations, ICLR 2023, Kigali, Rwanda, May 1-5, 2023*. OpenReview.net.

Yiming Wang, Pei Zhang, Baosong Yang, Derek F. Wong, and Rui Wang. 2025b. [Latent space chain-of-embedding enables output-free LLM self-evaluation](#). In *The Thirteenth International Conference on Learning Representations, ICLR 2025, Singapore, April 24-28, 2025*. OpenReview.net.

Jason Wei, Xuezhi Wang, Dale Schuurmans, Maarten Bosma, Brian Ichter, Fei Xia, Ed H. Chi, Quoc V. Le, and Denny Zhou. 2022. [Chain-of-thought prompting elicits reasoning in large language models](#). In *Advances in Neural Information Processing Systems 35: Annual Conference on Neural Information Processing Systems 2022, NeurIPS 2022, New Orleans, LA, USA, November 28 - December 9, 2022*.

Heming Xia, Yongqi Li, Chak Tou Leong, Wenjie Wang, and Wenjie Li. 2025. [Tokenskip: Controllable chain-of-thought compression in llms](#). *CoRR*, abs/2502.12067.

Chunlei Xin, Shuheng Zhou, Huijia Zhu, Weiqiang Wang, Xuanang Chen, Xinyan Guan, Yaojie Lu, Hongyu Lin, Xianpei Han, and Le Sun. 2025. [Sparse latents steer retrieval-augmented generation](#). In *Proceedings of the 63rd Annual Meeting of the Association for Computational Linguistics (Volume 1: Long Papers), ACL 2025, Vienna, Austria, July 27 - August 1, 2025*, pages 4547–4562. Association for Computational Linguistics.

An Yang, Anfeng Li, Baosong Yang, Beichen Zhang, Binyuan Hui, Bo Zheng, Bowen Yu, Chang Gao, Chengan Huang, Chenxu Lv, Chujie Zheng, Dayiheng Liu, Fan Zhou, Fei Huang, Feng Hu, Hao Ge, Haoran Wei, Huan Lin, Jialong Tang, and 40 others. 2025a. [Qwen3 technical report](#). *CoRR*, abs/2505.09388.

Zhen Yang, Mingyang Zhang, Feng Chen, Ganggui Ding, Liang Hou, Xin Tao, Pengfei Wan, and Ying-Cong Chen. 2025b. [Less is more: Improving LLM reasoning with minimal test-time intervention](#). *CoRR*, abs/2510.13940.

Qiying Yu, Zheng Zhang, Ruofei Zhu, Yufeng Yuan, Xiaochen Zuo, Yu Yue, Tiantian Fan, Gaohong Liu, Lingjun Liu, Xin Liu, Haibin Lin, Zhiqi Lin, Bole Ma, Guangming Sheng, Yuxuan Tong, Chi Zhang, Mofan Zhang, Wang Zhang, Hang Zhu, and 16 others. 2025. [DAPO: an open-source LLM reinforcement learning system at scale](#). *CoRR*, abs/2503.14476.

Andy Zou, Long Phan, Sarah Li Chen, James Campbell, Phillip Guo, Richard Ren, Alexander Pan, Xuwang Yin, Mantas Mazeika, Ann-Kathrin Dombrowski, Shashwat Goel, Nathaniel Li, Michael J. Byun, Zifan Wang, Alex Mallen, Steven Basart, Sanmi Koyejo, Dawn Song, Matt Fredrikson, and 2 others. 2023. [Representation engineering: A top-down approach to AI transparency](#). *CoRR*, abs/2310.01405.

A Preliminary Study of Probing

We conduct a preliminary probing study on mathematical reasoning benchmarks, including AIME and AMC-12. First, we construct contrastive datasets consisting of paired correct and incorrect reasoning trajectories for each input as described in §3.4. Then, using Qwen3 series models (1.7B and 4B), we extract last-token activation values across all layers as input features for probing classifiers. All samples are randomly partitioned into training and testing sets with a 4:1 ratio. Subsequently, we train a binary classifier to predict reasoning correctness from last-token activations. To mitigate the high dimensionality of the activation space, we apply F -statistic-based feature selection to identify the most discriminative neurons.

A.1 Data Construction

We utilize Qwen3-32B to generate contrastive reasoning trajectories. Specifically, starting from all AIME (24+25) and AMC-12 problems, we sample 8 reasoning traces per question using a generation temperature of 1.0. We retain only those questions that yield a balanced outcome of exactly 4 correct and 4 incorrect trajectories. Under this setting, we obtain 15 AIME problems (from an initial 60) and 13 AMC-12 problems (from an initial 104), resulting in 120 and 104 samples, respectively, for probing classifier training.

A.2 Preprocessing

For each reasoning trace, we extract last-token activations across all neurons as input features for the probing classifier. Specifically:

- **Source:** Hidden states of the last token in the reasoning path, immediately before final answer generation.
- **Position:** Post-activation outputs of the MLP blocks (i.e., after the SwiGLU activation for Qwen3 series model).
- **Dimension:** Activations from all transformer layers are concatenated into a single feature vector of dimension $L \times d_{\text{mlp}}$, where L denotes the number of layers.
- **Normalization:** Feature values are scaled by dividing by $10 \times \sigma$, where σ is the standard deviation for each neuron computed over the training set.

A.3 Probing Classifier

Given the high dimensionality of the activation space relative to the training sample size, feature selection is critical to mitigate overfitting. We rank neurons using the ANOVA F -statistic (`sklearn.f_classif`) based on their linear association with the correctness label, and select the top- K neurons with $K = 131,072$. For the probing classifier, we employed a Logistic Regression model with L1 regularization. The model was trained using 5-fold cross-validation with a stratified 4:1 train-test split.

The detailed settings are summarized in Table 6.

Table 6: Implementation details of probing classifier.

Setting	Configuration / Value
Feature	
Source	Last token of reasoning path
Position	MLP post-activation output
Scope	Global (all layers)
Normalization	Scaled by $1/(10 \times \text{std}_{\text{train}})$
Feature Selection	ANOVA F -statistic
Dimension of Input	131,072
Training	
Architecture	Logistic Regression (<code>sklearn</code>)
Regularization	L1 (Lasso)
Solver	SAGA
Class Weight	Balanced
Penalty Strength	Grid search $\in [10^{-4}, 10]$
Max Iterations	50
Random Seed	42
Validation	5-fold cross-validation
Metric	AUROC

B Detailed Data Statistics

B.1 Data for Adaptive Intervention Module

The adaptive intervention module is a binary classifier that predicts whether a given input is likely to fail under the base model and therefore requires intervention. Training data are constructed by sampling the base model on the training split for each benchmarks. Samples answered correctly are labeled as negative (i.e., no need for intervention), while incorrect samples are labeled as positive (i.e., intervention required). Dataset statistics are summarized in Table 7. Notably, for AMC-12 and HumanEval, we evaluate them only in a transfer setting using estimators trained on AIME and MBPP, due to lacking of training split; consequently, they are omitted from Table 7.

Table 7: Statistics of the training and validation data for the adaptive intervention module.

Dataset	Total Samples	Number of each label (Train / Val)	
		No Intervention	Need Intervention
AIME	828	392 / 99	270 / 67
MATH	1,000	622 / 270	78 / 30
GSM8K	1,700	1,097 / 459	103 / 41
MBPP	163	83 / 29	37 / 14

B.2 Data for Evaluation

We evaluate AdaRAS on a diverse set of benchmarks, where the dataset statistics are summarized in Table 8. All datasets are publicly available. Specifically, GSM8K, MATH, MBPP, and HumanEval are distributed under open licenses (i.e., MIT or Apache 2.0). The AIME and AMC datasets are sourced from public academic benchmarks widely accepted for evaluating mathematical reasoning. We split the datasets as follows:

- **AIME.** A unified set of samples is applied across all AIME datasets (2024, 2025, and Extend). This set contains 15 held-out samples (7 from AIME-24 and 8 from AIME-25), which are strictly excluded from all evaluation sets.
- **AMC-12, HumanEval.** Since these datasets do not provide official training splits, we reserve a small subset from the test split for performing AdaRAS. For example, we hold out 15 HumanEval samples for RCNs identification and evaluate on the remaining 149 samples.
- **Other datasets.** For benchmarks with official training splits (GSM8K, MATH, MBPP), patterns are extracted exclusively from the training set.

C Details of Implementation

We use the following hyperparameters for AdaRAS in main experiments:

- **Number of top- K neurons.** The number of intervened neurons is fixed to $K = 50$. As shown in Figure 5, these neurons are distributed across layers, with a higher concentration in middle-to-late layers.
- **Steering strength (α).** The best steering strength coefficient α is searched ranging $[0.1, 0.3]$.

All experiments are conducted on 4 NVIDIA A100 GPUs and 8 NVIDIA RTX 3090 GPUs.

C.1 Adaptive Intervention Module

we adopt a lightweight attention-based classifier for adaptive intervention module. Instead of using only the last token, this module take all token activations via an attention pooling mechanism to capture the global reasoning state. Detailed specifications are provided in Table 9.

C.2 Evaluation

To ensure fair comparison and reproducibility, we use greedy decoding during inference across all benchmarks.

Mathematic Benchmarks. For the AIME, MATH-500, GSM8K, and AMC-12 datasets, we use the following prompt:

User: Question: {question}
Thinking process:
Please provide a step-by-step thinking process and put your final answer in \boxed{ }.

Coding Benchmarks. For the HumanEval and MBPP datasets, we use the following prompt:

User: {question}

We employed the EvalPlus (Liu et al., 2023) library to safely extract and execute code blocks.

D Details of Reasoning Features

In Section 5.2, we use two trajectory-level metrics, Magnitude (\bar{M}) and Angle (\bar{A}), to analyze the geometric properties of reasoning trajectories in latent space. As in Figure 6, each point in the kernel density estimation (KDE) plot corresponds to the aggregated (\bar{M}, \bar{A}) values of a single complete reasoning trace. These metrics characterize the curvature and directional consistency of representation evolution across layers. Hidden states $\mathbf{h} \in \mathbb{R}^d$ are extracted from the model for each input, and the analysis is performed exclusively on generated reasoning tokens, excluding the input prompt. Following Wang et al. (2025b), the formal definitions are as follows:

Sequence-Averaged Magnitude (\bar{M}). This metric measures the “tortuosity” of the reasoning trajectory in the activation space. It is defined as the ratio of the accumulated layer-wise changes to the

Table 8: Statistics of datasets. #Probe indicates the number of samples used for identifying RCNs by AdaRAS.

Dataset	#Probe	#Test	Test split
Mathematic			
AIME-24 ¹	7	23	Self-split
AIME-25 ²	8	22	Self-split
AIME-Extend ³	15	150	Official
MATH-500 ⁴ (Lightman et al., 2024)	15	500	Official
GSM8K ⁵ (Hendrycks et al., 2021)	15	1,319	Official
AMC-12 ⁶	13	91	Self-split
Coding			
HumanEval ⁷ (Chen et al., 2021)	15	149	Self-split
HumanEval+ ⁸ (Liu et al., 2023)	15	149	Self-split
MBPP ⁹ (Austin et al., 2021)	15	378	Official
MBPP+ ¹⁰ (Liu et al., 2023)	15	378	Official

¹ https://huggingface.co/datasets/Maxwell-Jia/AIME_2024
² <https://huggingface.co/datasets/opencompass/AIME2025>
³ <https://www.kaggle.com/datasets/hemishveeraboina/aime-problem-set-1983-2024>
⁴ <https://huggingface.co/datasets/HuggingFaceH4/MATH-500>
⁵ <https://huggingface.co/datasets/openai/gsm8k>
⁶ https://huggingface.co/datasets/rulins/amc12_22-24
⁷ https://huggingface.co/datasets/openai/openai_humaneval
⁸ <https://huggingface.co/datasets/evalplus/humanevalplus>
⁹ <https://huggingface.co/datasets/google-research-datasets/mbpp>
¹⁰ <https://huggingface.co/datasets/evalplus/mbppplus>

Table 9: Architecture details for the adaptive intervention module.

Setting	Configuration
Architecture	
Structure	Linear(256, 256) → ReLU → Dropout(0.3) → Linear(256, 1)
Training	
Feature Selection	ANOVA F -statistic
Dimension of Input	256
Optimizer	Adam (LR=10 ⁻⁴ , Weight Decay=10 ⁻⁵)
Loss Function	BCEWithLogitsLoss
Epochs	100 (Early Stopping Patience=10)

net change from the first to the last layer. For a single token t , the magnitude score \mathcal{M}_t is computed as the L_2 -norm of the difference vector between adjacent layers, normalized by the global displacement:

$$\mathcal{M}_t = \frac{1}{L} \cdot \frac{\sum_{l=0}^{L-1} \|\mathbf{h}_t^{l+1} - \mathbf{h}_t^l\|_2}{\|\mathbf{h}_t^L - \mathbf{h}_t^0\|_2 + \epsilon}, \quad (4)$$

where $\epsilon = 10^{-6}$ is a small constant for numerical stability. The final sequence-averaged metric is

obtained by averaging over all generated tokens:

$$\bar{\mathcal{M}} = \frac{1}{T} \sum_{t=1}^T \mathcal{M}_t. \quad (5)$$

A lower $\bar{\mathcal{M}}$ indicates a straighter, more direct transformation of representations through the network depth, which we associate with more stable reasoning.

Sequence-Averaged Angle ($\bar{\mathcal{A}}$). This metric captures the directional stability of the semantic evolution. It calculates the angular deviation between adjacent layers relative to the global angular shift. We first define the cosine similarity $\text{sim}(\mathbf{u}, \mathbf{v}) = \frac{\mathbf{u} \cdot \mathbf{v}}{\|\mathbf{u}\| \|\mathbf{v}\|}$. The angle score \mathcal{A}_t for token t is defined as:

$$\mathcal{A}_t = \frac{1}{L} \cdot \frac{\sum_{l=0}^{L-1} \arccos \left(\text{sim}(\mathbf{h}_t^l, \mathbf{h}_t^{l+1}) \right)}{\arccos \left(\text{sim}(\mathbf{h}_t^0, \mathbf{h}_t^L) \right) + \epsilon}. \quad (6)$$

Similarly, the sequence-averaged angle is computed as:

$$\bar{\mathcal{A}} = \frac{1}{T} \sum_{t=1}^T \mathcal{A}_t. \quad (7)$$

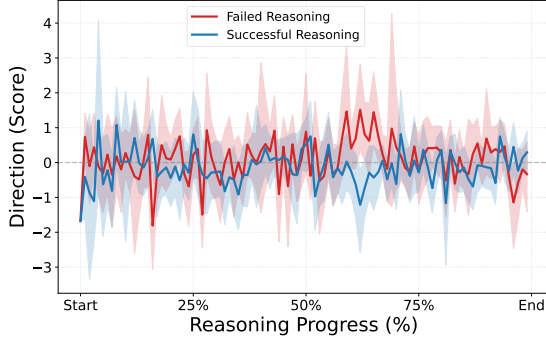


Figure 7: Projection of reasoning states onto the probing classifier learned space. The clear separation between **successful** (Blue) and **failed** (Red) trajectories validates the separability of reasoning correctness in the activation space.

Larger values of $\bar{\mathcal{M}}$ or $\bar{\mathcal{A}}$ imply that the reasoning process undergoes significant fluctuations or detours in the latent space.

E Additional Analysis Experiments

E.1 Separability of Reasoning Trajectories in Latent Space

To further validate the motivation that correct and incorrect reasoning exhibit distinct activation patterns, we visualize the evolution of latent representations. We use the weights of the linear probing classifier trained in §2.2 to define a reference direction. Specifically, we projected the layer-wise hidden states of reasoning traces onto the direction defined by the top- K most discriminative neurons identified by the probe.

Figure 7 illustrates the aggregated trajectories for successful and failed reasoning samples on the AIME dataset. The distinct separation between the two plots demonstrates that the latent reasoning states are linearly separable to a significant extent. Successful traces consistently maintain a high projection score, indicating stable alignment with the “correct” reasoning subspace learned by the probe. In contrast, failed traces exhibit high variance and downward drifts. This separability confirms that extracting reasoning-critical signals from activation patterns is feasible.

E.2 Empirical Result of Polarity of Neuron Activations

In Section 3.2, we proposed a polarity-based filtering method: constructing the steering vector by retaining only neurons that exhibit discriminative sign flips between correct and incorrect traces. To

verify the necessity of this strategy, we conducted an additional ablation study on the AIME benchmarks. We compare our method against a baseline selection strategy (“Magnitude Only”) that selects the Top- K neurons solely based on the absolute importance score $|S(l, i)|$, without enforcing the polarity constraint.

Table 10 presents the results. While selecting neurons based on magnitude alone yields performance gains over the base model (e.g., improving AIME-24 from 47.83% to 56.52%), introducing the polarity-aware filter significantly amplifies these gains. Specifically, our method achieves 60.87% on AIME-24 and 54.55% on AIME-25, consistently outperforming the magnitude-based selection. These results empirically confirm that neurons exhibiting contradictory activation patterns (sign flips) are important for reasoning validity, justifying our construction of S'_l .

Table 10: Effectiveness of polarity-based filtering. “Magnitude Only” selects top-50 neurons solely based on importance scores without polarity filtering.

Dataset	Accuracy (%)		
	Base	Magnitude Only	Polarity-Aware (Ours)
AIME-24	47.83	56.52	60.87
AIME-25	40.91	45.45	54.55
AIME-Extended	47.33	50.67	52.67

F Case Study

To intuitively understand how AdaRAS corrects reasoning errors, we present three randomly selected examples from the AIME dataset. In each case, we compare the reasoning trace generated by the base model (which fails) against the trace generated with our sparse activation steering. Blue text highlights the **correct logical steps** induced by AdaRAS, while red text indicates the **errors or hallucinations** in the base model’s reasoning.

Case 1: Correcting Domain Constraints in Geometry

Problem: Let A, B, C, D be points on the hyperbola $\frac{x^2}{20} - \frac{y^2}{24} = 1$ such that $ABCD$ is a rhombus whose diagonals intersect at the origin. Find the greatest real number that is less than BD^2 for all such rhombi.

Comparison of Reasoning Traces

Base Model (Failed):

... We derive the expression for the diagonal squared as $BD^2 = 80 + \frac{22}{3}d^2$. Since $d^2 \geq 0$, the expression is always greater than 80. As $d \rightarrow 0$, BD^2 approaches 80. Therefore, the greatest real number less than BD^2 is [80].

AdaRAS (Success):

... We derive the expression $BD^2 = 80 + \frac{22}{3}d^2$. However, the vertices must lie on the hyperbola. Solving the system for the rhombus vertices $(c, 0)$ and $(0, d)$ yields the constraint that d^2 cannot be zero. Specifically, the minimum value is found to be $d^2 = \frac{600}{11}$. Substituting this into the expression: $BD^2 = 80 + \frac{22}{3} \cdot \frac{600}{11} = 480$. Thus, the greatest real number is [480].

Analysis: In this geometry problem, the Base model correctly derives the algebraic formula but fails to check the *geometric domain constraints* (it assumes d can be arbitrarily small). AdaRAS steers the model to verify the existence condition of the rhombus, identifying the lower bound of d^2 implied by the hyperbola's equation. This illustrates that our steering vector encodes signals related to “constraint satisfaction.”

Case 2: Rectifying Symbolic Manipulation

Problem: Evaluate the product:

$$\prod_{k=4}^{63} \frac{\log_k(5^{k^2-1})}{\log_{k+1}(5^{k^2-4})}.$$

Find $m + n$ where the result is m/n .

Comparison of Reasoning Traces

Base Model (Failed):

... We simplify the general term. The rational part telescopes to $\frac{31}{13}$. For the logarithmic part, we consider $\prod \log_{k+1} k$. This product telescopes to $\frac{1}{\log_4 64} = \frac{1}{3}$. Multiplying the results yields $\frac{31}{13} \cdot \frac{1}{3} = \frac{31}{39}$. Thus $m + n = [70]$.

AdaRAS (Success):

... We simplify the general term using logarithmic identities: $\frac{\log_k(5^{k^2-1})}{\log_{k+1}(5^{k^2-4})} \rightarrow \dots \rightarrow \log_k(k+1)$. We split the product. The rational part is $\frac{31}{13}$. The logarithmic part is $\prod_{k=4}^{63} \log_k(k+1)$. Using the change of base formula $\log_k(k+1) = \frac{\ln(k+1)}{\ln k}$, this telescopes to $\frac{\ln 64}{\ln 4} = \log_4 64 = 3$. Multiplying the results gives $\frac{31}{13} \cdot 3 = \frac{93}{13}$. Summing them yields [106].

Analysis: Here, the Base model performs a valid rational simplification but hallucinates the result of

the logarithmic telescoping product (calculating it as $1/3$ instead of 3, effectively inverting the base and argument). AdaRAS corrects this symbolic manipulation error, guiding the model to apply the change-of-base formula correctly.

Case 3: Deriving Correct Geometric Relationships

Problem: Circle ω_1 (radius 6) is internally tangent to ω_2 (radius 15). A rectangle $EFGH$ is inscribed in ω_1 such that specific area conditions are met. Find the area of $EFGH$.

Comparison of Reasoning Traces

Base Model (Failed):

... Let the vertices be (a, b) . Equating the areas of $\triangle DGF$ and $\triangle CHG$ yields the condition $|a(12 - b)| = |b(24 + a)|$. Simplifying this leads to the relationship $b = \frac{6a}{a+12}$. Substituting this into the circle equation and solving... yields an area of 48. Final Answer: [49].

AdaRAS (Success):

... Let the rectangle dimensions be determined by coordinate y and width m . Equating the areas of $\triangle DGF$ and $\triangle CHG$ leads to the equation $12m - my = 48y - my$. The term $-my$ cancels out, simplifying to $12m = 48y$, which implies $m = 4y$. Substituting this into the circle constraint $(m/2)^2 + y^2 = 36 \implies 5y^2 = 36$. The area is $m \cdot 2y = 8y^2 = \frac{288}{5}$. Final Answer: [293].

Analysis: The Base model sets up the coordinate geometry correctly but fails at the algebraic simplification step, hallucinating a complex rational relationship ($b = \frac{6a}{a+12}$) that does not follow from the area equality. AdaRAS successfully recovers the linear relationship ($m = 4y$) by correctly canceling terms during the derivation, ensuring the subsequent area calculation is based on valid premises.